❏   1732

DTC-SVM Control for Permanent Magnet Synchronous Generator based Variable Speed Wind Turbine

El Mourabit Youness[1], Derouich Aziz[2], El Ghzizal Abdelaziz[3], El Ouanjli Najib[4], Zamzoum Othmane[5]
Laboratory of Production Engineering, Energy and Sustainable Development, Higher School of Technology, Sidi Mohamed Ben Abdellah University Fez, Morocco

Article Info	ABSTRACT
	In this paper, we are interested in improving the production efficiency for electric energy extracted from a wind turbine, based on a permanent magnet synchronous generator (PMSG) that we want to improve the performance by means of direct torque control with space vector modulation (DTC-SVM). The choice of this control comes from the deficiencies inherent to the conventional DTC, which includes variable switching frequency, torque ripple and implementation complexity. First we focus on the wind energy conversion system (WECS) modeling using the PMSG machine, as well as the detailed study for the control DTC-SVM operating principle. Then, system performance is tested and compared by simulation in the MATLAB/Simulink in terms of follow instructions, robustness to the variations of the external system elements, and effectiveness of the expected method.

Corresponding Author:

El Mourabit Youness,
Laboratory of Production Engineering, Energy and Sustainable Development,
Sidi Mohamed Ben Abdellah University,
Higher School of Technology, BP 2427, Rte Imouzzer, Fez, Morocco.
Email: Youness.elmourabit@usmba.ac.ma

1. INTRODUCTION

Wind energy is considered among the best clean and renewable natural resources. Indeed, the degradation of the ecological environment for the electrical energy production using conventional means makes wind power production more efficient to replace the standard production chains. [1]-[2]. The WECS system based on a variable wind speed system that incorporates direct drive permanent magnet synchronous machine is becoming a current trend in this area, as a better energy capture, reduced mechanical stress, increased efficiency and reliability [3].

According to [3] a 15% increase in energy captured is achieved using variable wind speed system with reference to a fixed speed system, in the same context, and if we neglect the losses in the electronic power converter we can reach a rate of 15 to 23% of the energy obtained according to [4]. Another important argument for using variable speed strategies is specific wind sites. Whereas a fixed speed system is designed to be site specific, operating nearest the maximum power [5], variable speed systems are handy and generic system can be employed at a wider range for the different wind sites.

The use of wind energy generation has mainly been dominated by the induction generator (IG), and more especially the doubly fed induction generator (DFIG), with a converter attached to the rotor windings [6]. Though this last time, the incorporation of PMSG has become an increasingly attractive alternative [7].The use of an IG in a WECS requires a gearbox, due to the high nominal rotational speeds of IGs as compared to the slow rotational speeds for the wind turbine. It is desirable to do away with the high weight, mechanical losses, costs and maintenance requirements of gearboxes. The integration of PMSGs in these applications addresses this problem because PMSGs with a high number of poles operate at much lower

speeds, eliminating the need for gearboxes [8]-[9]. A gear-less WECS is commonly referred to as being direct-drive.

Make use of a full- scale back-to-back power converter as depicted on (fig.1) is considered among the best topologies of power electronics used in the WECS [10]-[11]. The DTC application to WECSs is a relatively new concept, this control strategy was introduced by Takahashi [12] and Depenbrock [13]. In [14] and [15] it's concluded that because of its insensitivity to physical parameters, inherent sensorless operation and ease in implementing variable speed strategies, DTC is more suited in WECSs than the classic Field Oriented Control (FOC). The aim of this work is the modelling and implementation of a complete position sensorless WECS, incorporating direct torque control through space vector modulation (DTC-SVM) of a permanent magnet synchronous generator.

2. WIND ENERGY CONVERSION SYSTEM MODELING
2.1. Wind Turbine modeling
The proposed system, that is believed to satisfy the description given, is presented in Figure 1.
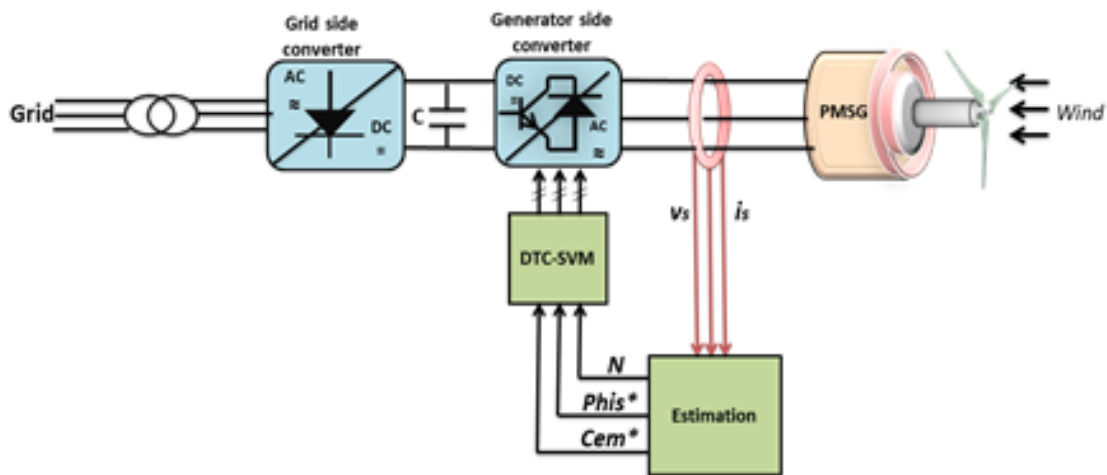

Figure 1. Representation of the system to be designed

The wind turbine and its interaction with the environment is an extremely complex system. A very good indepth analysis of the mechanical modeling of wind turbine models can be found in [16]. According to Betz's theory of aerodynamics, the input power of the wind turbine can be defined as follows.

$$P_m = \frac{1}{2} C_p(\lambda, \beta). \rho. S. V_{v^3} \tag{1}$$

$$\lambda = \frac{R.\Omega}{V_v} \tag{2}$$

The tip speed ratio (TSR) represents the ratio of wind speed to turbine rotational speed. This quantity is defined in (2) and is of importance when considering the turbine blade power characteristics.
The wind torque is proportional to the square of the angular speed of the rotor:

$$C_{éol} = \frac{1}{2}. \frac{C_p(\lambda).\rho.S.R^3}{\lambda^3}. \Omega^2 \tag{3}$$

By placing in the optimal operating conditions of the wind turbine $\lambda = \lambda_{opt}$, the ratio of the angular speed and torque to have the maximum of the power is given by the relationship

$$C_{éol}^{opt} = \frac{1}{2}. \frac{C_{pmax}(\lambda).\rho.S.R^3}{\lambda_{opt}^3}. \Omega^2 \tag{4}$$

The total mechanical torque delivered by the wind turbine is given by:

$$C_m = \frac{P_m}{\Omega} \tag{5}$$

$$C_m = \frac{1}{2}\,\rho.\pi.R^3.\frac{C_p(\lambda,\beta)}{\lambda} \tag{6}$$

Several numerical approximations have been developed in the literature to determine an expression of the coefficient C_P. We have put the following formula:

$$Cp(\lambda,\beta) = 0.5176\left(\frac{116}{\lambda'} - 0.4\beta - 5\right)e^{\frac{-21}{\lambda'}} + 0.0068\lambda \tag{7}$$

$$\frac{1}{\lambda'} = \frac{1}{\lambda+0.08\beta} - \frac{0.035}{\beta^3+1} \tag{8}$$
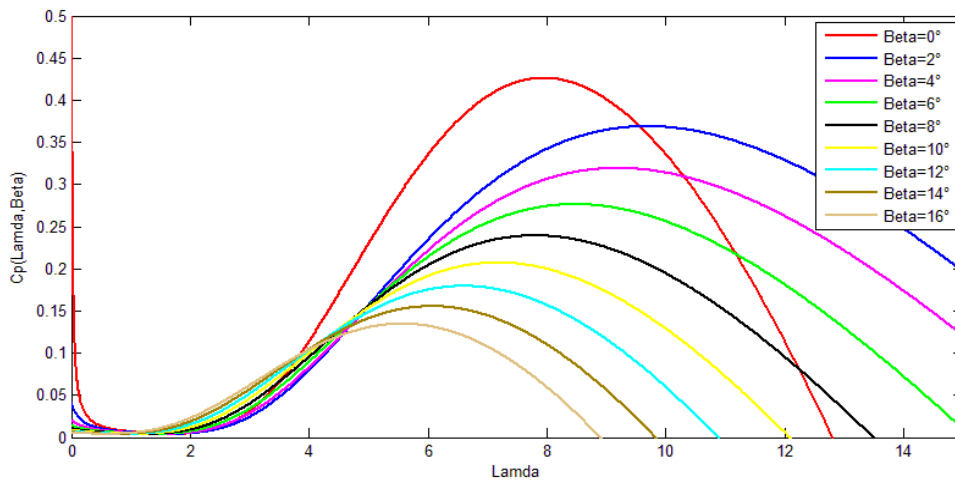

Figure 2. Power coefficient Cp for constant values of β

2.2. PMSG modeling

The model of the permanent magnet wind generator after the Park transformation is defined by the electrical, magnetic and mechanical following equations:

$$\begin{cases} V_{sd} = -R_s.i_{sd} + \frac{d\varnothing_d}{dt} - \omega_r.\varnothing_q \\ V_{sq} = -R_s.i_{sq} + \frac{d\varnothing_q}{dt} + \omega_r.\varnothing_d \end{cases} \tag{9}$$

The totalized fluxes in each phase are as follows:

$$\begin{cases} \varnothing_d = -L_d.i_{sd} + \varnothing_f \\ \varnothing_q = -L_q.i_{sq} \end{cases} \tag{10}$$

This allows the electrical equations to be written as follows:

$$\begin{cases} V_{sd} = -R_s.i_{sd} + \frac{d(-L_d.i_{sd}+ \varnothing_f)}{dt} - \omega_r.\left(-L_q.i_{sq}\right) \\ V_{sq} = -R_s.i_{sq} + \frac{d(-L_q.i_{sq})}{dt} + \omega_r.\left(-L_d.i_{sd} + \varnothing_f\right) \end{cases} \tag{11}$$

After transformation and simplification, we have:

$$\begin{cases} V_{sd} = -R_s.i_{sd} - L_d \frac{d(i_{sd})}{dt} + \omega_r.(L_q.i_{sq}) \\ V_{sq} = -R_s.i_{sq} - L_q \frac{d(i_{sq})}{dt} - \omega_r.(L_d.i_{sd}) + \omega_r.\emptyset_f \end{cases} \tag{12}$$

Equation 12 can be written as follows:

$$\begin{cases} V_{sd} = -R_s.i_{sd} - L_d \frac{d(i_{sd})}{dt} + e_q \\ V_{sq} = -R_s.i_{sq} - L_q \frac{d(i_{sq})}{dt} - e_d + E_{q0} \end{cases} \tag{13}$$

With:

$$\begin{cases} e_d = \omega_r.(L_d.i_{sd}) \\ e_q = \omega_r.(L_q.i_{sq}) \\ E_{q0} = \omega_r.\emptyset_f \end{cases} \tag{14}$$

The mechanical equations are described:

$$\begin{cases} C_{em} = {^3\!/_2}.p.[(L_d - L_q).I_{sd}.I_{sq} - I_{sq}.\emptyset_f] \\ C_{\acute{e}ol} - C_{em} = J.\frac{d\Omega}{dt} + f_c.\Omega \end{cases} \tag{15}$$

3. DIRECT TORQUE CONTROL
3.1. The DTC control principle

      The direct torque control (DTC) based on the orientation of the stator flow uses the instantaneous values of the voltage vector. A three-phase converter can provide eight instantaneous basic voltage vectors, of which two are zero [17]-[18]. These vectors are chosen from a switching table as a function of the flux and torque errors and the position of the stator flux vector.

The voltage vector Vs can be written:

$$V_s = \sqrt{\frac{2}{3}} U_{DC}\{S_a + S_b e^{j\frac{2\pi}{3}} + S_c e^{j\frac{4\pi}{3}}\} \tag{16}$$

- $S_{i(i=1,3,|5)} = 0$ if the high switch is closed and the low switch is open.
- $S_{j(j=2,4,|6)} = 1$ if the high switch is closed and the low switch is closed.

3.2. Space Vector Modulation

      The theory and operation principle of space vector modulation (SVM) is mostly adapted from. SVM is an alternative inverter switch control method to traditional sinusoidal PWM, over which it has many advantages. Control structures are greatly simplified and power electronic hardware is exploited to the maximum. SVM inherently realises third harmonic injection, increasing the maximum output voltage of the inverter. Important characteristics for the implementation of SVM are that there must be a single DC source to the converter. SVM is realised in the stationary reference frame, as depicted in Figure 3.

      The voltage vectors and their relationship to the converter in Figure 3 are given in Table 1. The top level switches of the converter (S_1, S_3 and S_5), and the bottom level switches (S_2, S_4 and S_6) switch complimentary. In the table, a 0 represents an open or off switch, while a 1 represents a closed or on switch.

The α,β plane as shown in Figure 3, is divided up into six aqual sectors, these voltage vectors are the only eight possible outputs of this topology of converter. The reference voltage $V_{\alpha\beta}$, which is the desired voltage at the inverter terminals, rotates in the α,β plane at a certain angular frequency, with angle θ. This voltage vector is then projected as T_3 and T_4 shown in Figure 3 onto the voltage vectors enclosing the current sector.
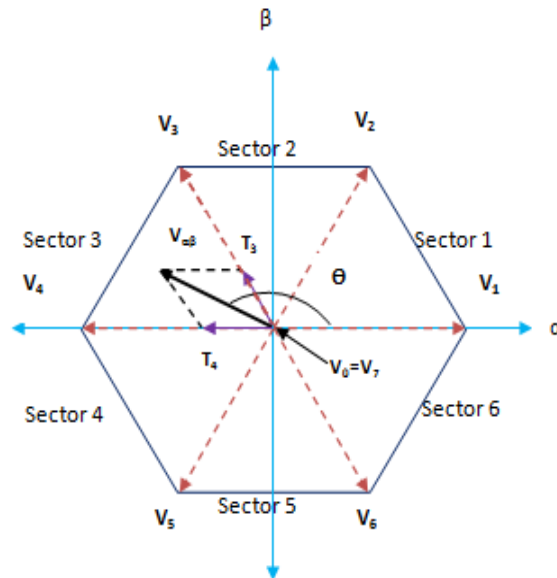
Figure 3. Reference frame of the operation principle of space vector modulation

Table 1. SVM voltage vectors and the implications on converter switching and output voltages

Vector	S_1	S_3	S_5	S_2	S_4	S_6	V_a	V_b	V_c
V_0	0	0	0	1	1	1	0	0	0
V_1	1	0	0	0	1	1	V_{dc}	0	0
V_2	1	1	0	0	0	1	V_{dc}	V_{dc}	0
V_3	0	1	0	1	0	1	0	V_{dc}	0
V_4	0	1	1	1	0	0	0	V_{dc}	V_{dc}
V_5	0	0	1	1	1	0	0	0	V_{dc}
V_6	1	0	1	0	1	0	V_{dc}	0	V_{dc}
V_7	1	1	1	0	0	0	V_{dc}	V_{dc}	V_{dc}

The projections will then ultimately determine the duty cycles of the power electronic switches. The size of the projection vectors determine the amount of time that the switches spend in a certain switching state for each switching period. An example timing diagram of one such switching period is given in Figure 5 to illustrate this. The order in which the boundary vectors are switched in a specific switching period can be arbitrarily chosen, as long as the total switching time of a vector remains the same in any sequence. Note that V_0 and V_7 are the zero vectors, and can be interchangeably used.
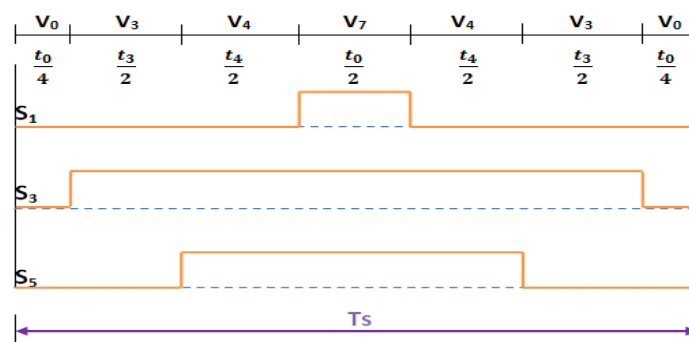

Figure 4. Representation of one switching period of SVM

The reference voltage vector is in sector 3, as in the vector diagram in Figure 3. From Figure 3 it can be seen that each voltage vector is switched for a certain time. These times can easily be calculated as:

$$\begin{cases} t_3 = \frac{|T_3|}{|V_3|}.T_s \\ t_4 = \frac{|T_4|}{|V_4|}.T_s \\ t_0 = T_s - t_3 - t_4 \end{cases} \qquad (17)$$

3.3.   Direct Torque Control with Space Vector Modulation
3.3.1. Flux linkage control

DTC-SVM has many advantages that strongly support the application thereof in this system. Most importantly, these advantages include [19]:

- Direct control over electromagnetic torque, which allows for easy implementation of maximum power point tracking strategies in wind energy conversion system.
- Requires a lower switching frequency, especially when compared to classical DTC.
- Offers very good speed control performance, which is a component of the WECS.

The following equations presents the relationship between the voltage vectors and the stator flux vectors of the PMSG:

$$\vec{\emptyset_s}(t) = \int_0^{t_e}(\vec{V_s} - R_s.\vec{I_s}).dt + \vec{\emptyset_{s0}} \qquad (18)$$

If it is assumed that the stator resistance is small enough, the voltage drop across the resistance becomes neglected in front of V_s. The calculation of the integral in the interval [0, t_e] gives:

$$\vec{\emptyset_s} = \vec{V_s}.t_e + \vec{\emptyset_{s0}} \qquad (19)$$

In a global way, it can be considered that:

$$\vec{\emptyset}_{s(k+1)} = \vec{V_s}.t_e + \vec{\emptyset}_{s(k)} \qquad (20)$$

With:

$\vec{\emptyset}_{s(k)}$: Vector of the flux in the step of current sampling

$\vec{\emptyset}_{s(k+1)}$: Vector of the flow of the next step of the sampling.

t_e : Sampling period

3.3.2. The electromagnetic torque Control:

The electromagnetic torque developed by the PMSG, in terms of dq-frame variables, can be expressed by the following equation:

$$C_{em} = \frac{3}{2}p\left(\frac{|\vec{\emptyset_s}|\emptyset_f \sin\delta}{L_d} - \frac{|\vec{\emptyset_s}|^2(L_d-L_q)\sin 2\delta}{2L_dL_q}\right) \qquad (21)$$

When a non-salient PMSG is considered, and we equate the static stator inductance to L_s, the expression in (21) reduces to:

$$C_{em} = \frac{3}{2}p\left(\frac{|\vec{\emptyset_s}|\emptyset_f \sin\delta}{L_d}\right) \qquad (22)$$

The principle of DTC can be deduced from (22), the electromagnetic torque C_{em} of the synchronous machine can be directly controlled by varying the torque angle δ, also referred to previously as the power angle, which is actually the angle difference between the PM rotor field and the rotating stator flux linkage. The torque angle can therefore be controlled by varying the stator flux angle. According to (19) we have the relation. It is clear that the adjustment of the PMSG terminal voltage $V_{s,\alpha\beta}$ has a direct effect on the derivative of the stator flux linkage .The appropriate voltage vector is then selected by the SVM, and DTC-SVM is realised. The basic configuration of DTC with Space Vector Modulation, or DTC-SVM, is presented in Figure 5.

$$\frac{d\vec{\emptyset_{s,\alpha\beta}}}{dt} = \vec{V_{s,\alpha\beta}} - R_s\vec{I_{s,\alpha\beta}} \qquad (23)$$
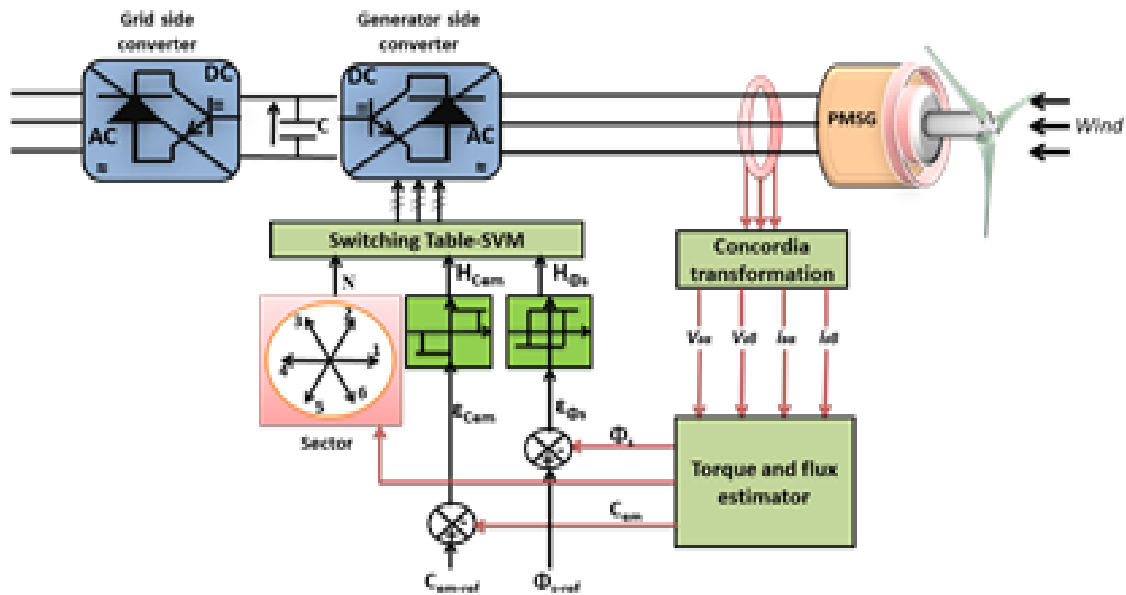
Figure 5. General structure of the DTC-SVM applied to the PMSG

3.3.3. Estimation of the flux and the torque
The electromagnetic torque is estimated by:

$$C_{em} = \frac{3}{2}p.(\emptyset_{s\alpha}.i_{s\beta} - \emptyset_{s\beta}.i_{s\alpha}) \tag{24}$$

The flux is estimated by:

$$\emptyset_s = \emptyset_{s\alpha} + j.\emptyset_{s\beta} \tag{25}$$

With:

$$\begin{cases} \emptyset_{s\alpha} = \int_0^t (V_{s\alpha} - R_s.i_{s\alpha}).dt \\ \emptyset_{s\beta} = \int_0^t (V_{s\beta} - R_s.i_{s\beta}).dt \end{cases} \tag{26}$$

To model in the complex plane (α,β) the different variables, vectors tensions, currents and flux we must put in disposition the transformation of Concordia:

$$\begin{pmatrix} x_\alpha \\ x_\beta \end{pmatrix} = \sqrt{\frac{2}{3}}.\begin{pmatrix} 1 & -\frac{1}{2} & -\frac{1}{2} \\ 0 & \frac{\sqrt{3}}{3} & -\frac{\sqrt{3}}{3} \end{pmatrix}.\begin{pmatrix} X_a \\ X_b \\ X_c \end{pmatrix} \tag{27}$$

With: X = V_s or i_s

3.3.4. General selection table for Direct Torque Control
From the following table it can be seen that the states V_k and V_{k+3} are not used in the torque evolution provided that they can be changed to the same sector in agreement with the evolution of the stator flux.

Table 2. General Selection table for Direct Torque Control

Voltage Vector	Increase			Decrease		
Stator flux	V_k	V_{k+1}	V_{k-1}	V_{k+2}	V_{k-2}	V_{k+3}
Torque		V_{k+1}	V_{k+2}		V_{k-1}	V_{k-2}

With   k: the sector number.
The state choice is made through the switching Table.3 [20].

Table 3. The switching table for the PMSG DTC drives

$H_{\Phi s}$	H_{Cem}	Sector 1	Sector 2	Sector 3	Sector 4	Sector 5	Sector 6
1	1	V_2(110)	V_3(010)	V_4(011)	V_5(001)	V_6(101)	V_1(100)
1	0	V_7(111)	V_0(000)	V_7(111)	V_0(000)	V_7(111)	V_0(000)
1	-1	V_6(101)	V_1(100)	V_2(110)	V_3(010)	V_4(011)	V_5(001)
0	1	V_3(010)	V_4(011)	V_5(001)	V_6(101)	V_1(100)	V_2(110)
0	0	V_0(000)	V_7(111)	V_0(000)	V_7(111)	V_0(000)	V_7(111)
0	-1	V_5(001)	V_6(101)	V_1(100)	V_2(110)	V_3(010)	V_4(011)

$H_{\Phi s}$ H_{Cem}: are the output of the flux regulator and the electromagnetic torque regulator.

4.   RESULTS AND DISCUSSION

The system is modeled in MATLAB/Simulink. The simulation results are presented and discussed. The global model is presented in Figure 6.
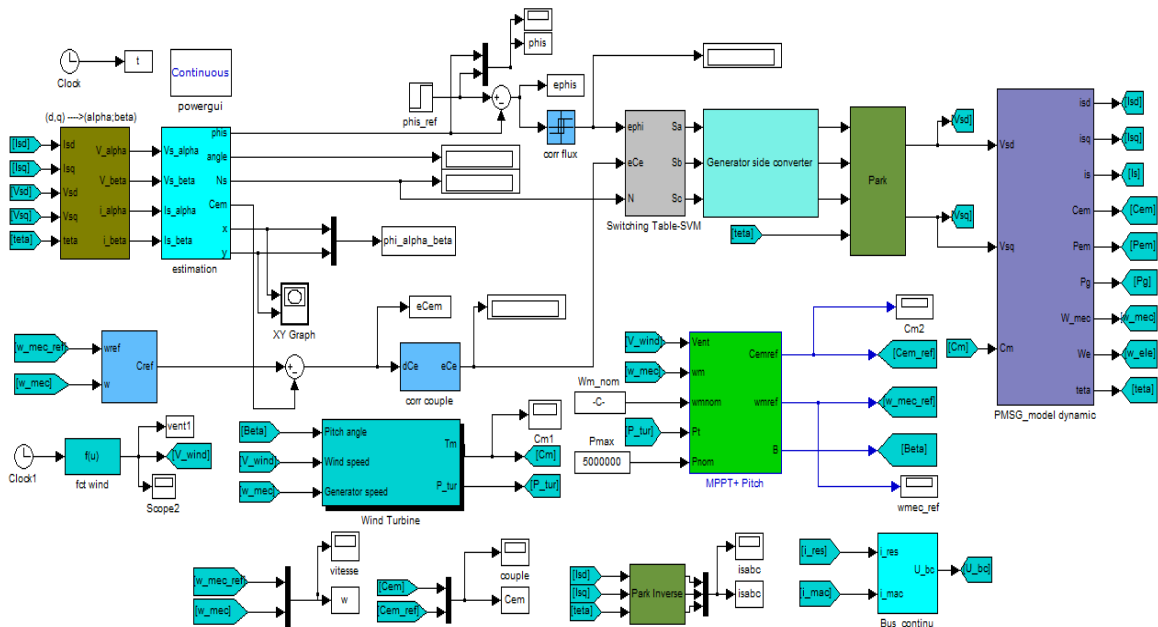

Figure 6. Simulation scheme of DTC control for PMSG in Matlab/Simulink

4.1. Simulation results

In this simulation we took the following values as references, the reference stator flux is of the order of $\emptyset_{s\_ref} = 4.5\ Wb$, the hysteresis comparator bandwidth of the stator flux it is of the order $\pm\ 0.0001$Wb, as well as hysteresis comparator bandwidth for torque is fixed in $\pm\ 0.01$N.m.

4.1.1. Optimal wind speed test

The figure (7.a) shows the wind profile and the figure (7.b) illustrates the angular speed evolution of machine. The figures (8.a and.8.b) show the evolution of the stator flux which remains constant at its reference value, the evolution of the stator flux in the complex reference frame (α, β) (fig.8.c) perfectly shows the circular trajectory. The figure (9.a) illustrates the evolution of the electromagnetic torque with its reference value, and the figure (9.b) shows the control result of the active and reactive power delivered by the machine. The curve of figure (9.c) shows the components of three-phase stator currents which have the sinusoidal shape with a frequency proportional to the rotation speed. Throughout the test, the system operates at unit power factor ($Q_{s\_res} = 0$).
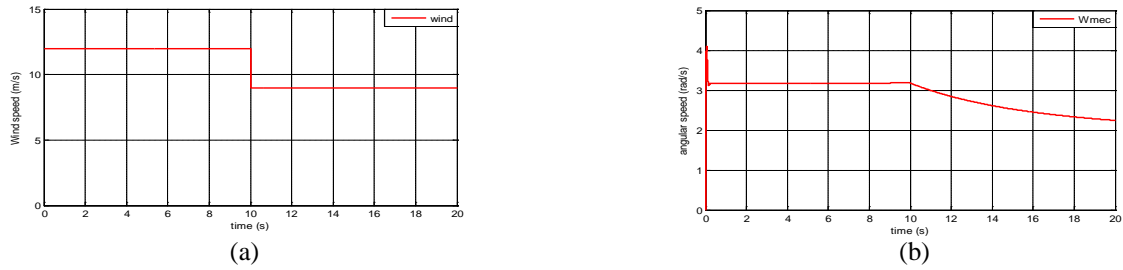
(a)

(b)

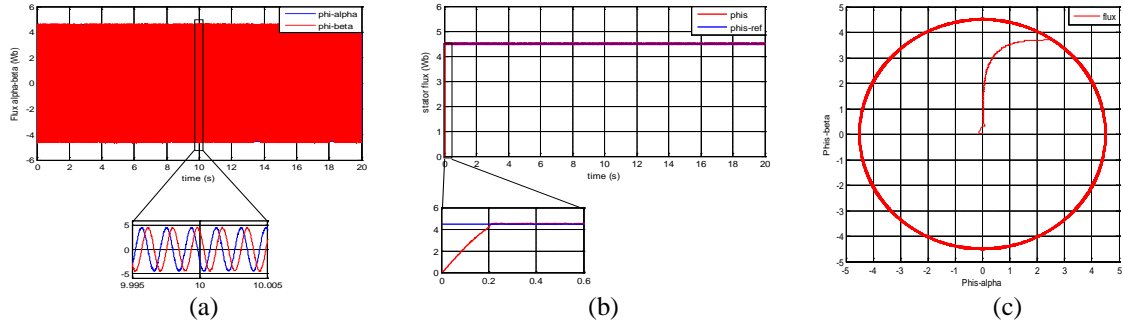Figure 7. Optimal wind speed test, (a) Wind profil, (b) angular speed

(a)

(b)

(c)

Figure 8. Optimal wind speed test, (a) stator flux alpha-beta, (b) stator flux, (c) evolution of the stator flux in the reference frame (α, β)
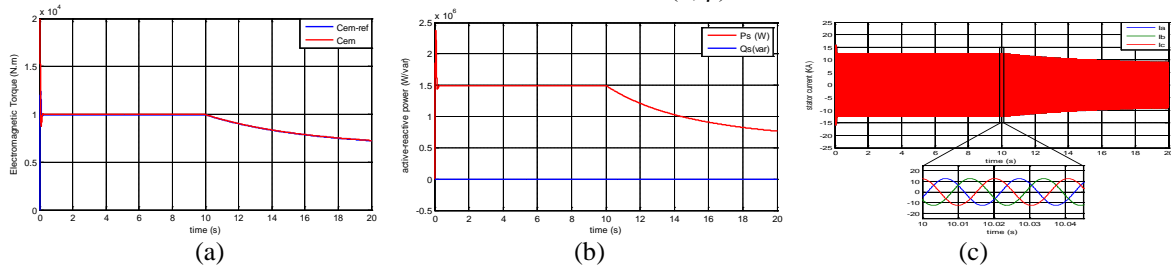

(a)

(b)

(c)

Figure 9. Optimal wind speed test, (a) Electromagnetic torque (b) active and reactive power, (c) Stator currents

4.1.2. Random wind speed test

The simulation is done to a wind profile as follows:

$$V_1(t) = 12 + 0.2 * sin(0.1047t) + 2 * sin(0.2665t) + sin(1.293t) + 0.2 * sin(3.6645t)$$

It has been observed since the test that the evolution of the stator flow perfectly follows the reference values even if in the presence of a variable wind, which means a perfect decoupling between the torque and the flux, which shows the efficiency and the robustness of the DTC control vis-à-vis the variation of external parameters as shown in the graphs of the Figure10,11 and 12.
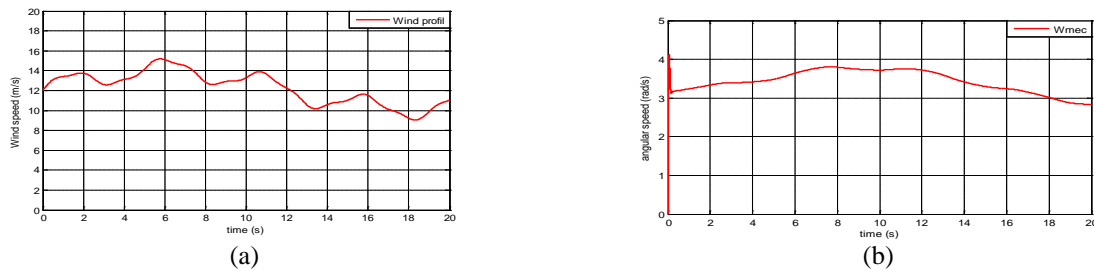

(a)

(b)

Figure 10. Random wind speed test, (a) Wind speed profile, (b) angular speed
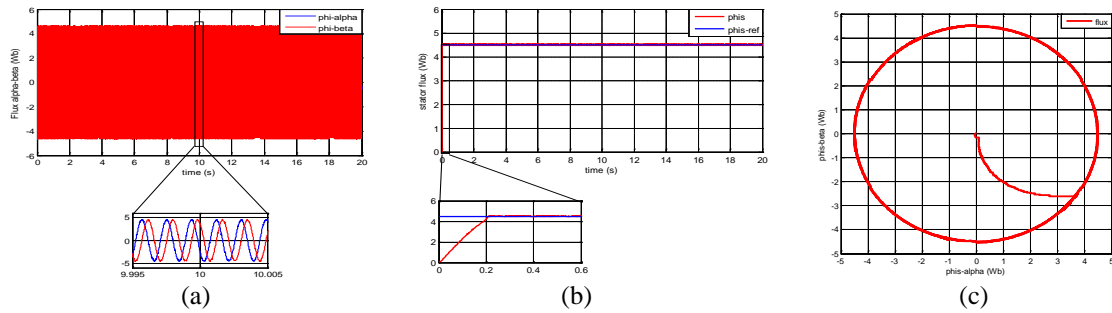
Figure 11. Random wind speed test, (a) stator flux in Concordia plan, (b) Stator flux with their reference, (c) evolution of the stator flux in the reference frame (α, β)
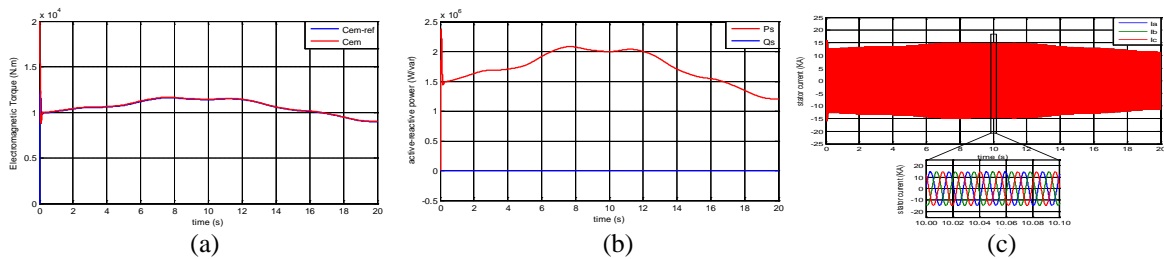

Figure 12. Random wind speed test (a) Electromagnetic torque (b) active and reactive power, (c) Stator currents

The inherent shortcomings of classic DTC, which include variable switching frequency, severe torque ripple and implementation complexity is overcome by implementing DTC-SVM. DTC-SVM has many advantages that strongly support the application thereof in this system. Most importantly, these advantages include:

1. Direct control over electromagnetic torque, which allows for easy implementation of maximum power point tracking strategies in wind energy conversion systems.
2. Requires a lower switching frequency, especially when compared to classical DTC.
3. Offers very good speed control performance, which is a component of the WECS.

5. CONCLUSION

The principal goals of this paper is to perform a modeling and to implement a complete position sensorless wind energy conversion system (WECS), incorporating DTC control with space vector modulation for à PMSG generator, this is why mathematical models of the system have been developed and the theory of the referential applied to the electrical model has been designed in order to obtain the models of fixed and rotation reference fram systems. The coordinate transformations are not only necessary to simplify the design and simulation of the system, but are required by the sub systems comprising the WECS, the DTC-SVM control method that is implemented in this system requires the system model to be expressed in the stator flux synchronously rotating reference frame.The control strategy proposed in this work has shown that it can manage the electromagnetic torque of the PMSG generator in order to provide the desired power and this according to the change in wind speed, the simulation results clearly shows the efficiency of the followed by instructions regarding the permanent changes of the external parameters. Although the application of DTC to WECS is a relatively new concept, the conclusion of this work agrees that DTC control is more suited to the control of WECSs than FOC.

APPENDIX

Table 4. Parameters of Permanent Magnet Synchronous Machine and wind turbine

Variable	Symbol	Value (unit)
Power Generator	P_n	1.5 MW
pair pole number	p	48
Stator Resistance	R_s	6.25e-3 Ω
d axis inductance	L_d	4.229e-3 H
q axis inductance	L_q	4.229e-3 H
Generator rotor flux	ϕ_f	11.1464 Wb
Coefficient of friction	f_c	0,0003035 N.m.s/rad
Turbine moment	J	10000 N.m
Specific density of air	ρ	1.22 kg/m3
Radius of the turbine blade	R	55m
power coefficient	Cp_{max}	0.35
tip-speed ratio	λ_{opt}	7.07

Nomenclature

Designation	Symbol	Unit
time	t	S
pitch angle	β	°
Power captured by the wind turbine	P_m	W
Blade swept area	S	m^2
Wind speed	V_v	m/s
Mechanical generator speed	Ω	Rpm
Turbine torque	$C_{éol}$	N.m
Optimal turbine torque	$C_{éol}^{opt}$	N.m
d–q axis stator voltage	V_{sd}, V_{sq}	V
d–q axis stator current	i_{sd}, i_{sq}	A
d-q axis flux	$\emptyset_d, \emptyset_q$	Wb
Electromagnetic generator torque	C_{em}	N.m
Stator voltage vector	V_s	V
Stator flux in the complex plane	$\emptyset_{s\alpha}, \emptyset_{s\beta}$	Wb
DC-link voltage	V_{DC}	V
Electric pulsation	ω_r	Rad/s

REFERENCES

[1]   K. Xie, *et al.*, "Energy and Reliability Benefits of Wind Energy Conversion Systems, " *Renewable Energy*, Vol. 36, pp. 1983-1988, No. 7, 2011.

[2]   R. Belu, *et al.*, "Wind Characteristics and Wind Energy Potential in Western Nevada, " *Renew. Energy* 34, pp. 2246–2251, 10, 2009.

[3]   H. Li, *et al.*, "Overview of Different Wind Generator Systems and their Comparisons," *IET Renewable Power Generation,* vol. 2, no. 2, pp. 123-138, 2008.

[4]   J. Stegmann, *et al.*, "Economic and Eciency Evaluation of Dierent Battery Charging Wind Generator Systems," *Southern African Universities Power Engineering Conference, Johannesburg, South Africa*, pp. 205-210, January 2010.

[5]   E. Muljadi, *et al.*, "A Conservative Control Strategy for Variable Speed Stall Regulated Wind Turbines," *ASME Wind Energy Symposium, Reno, NV, USA*, January 2000.

[6]   A. Derouich, *et al.*, "Real-Time Simulation and Analysis of the Induction Machine Performances Operating at Flux Constant*," International Journal of Advanced Computer Science and Applications*, vol/issue: 5(4), 2014.

[7]   S. A. Diaz, *et al.*, "Indirect Sensorless Speed Control of a PMSG for Wind Application," *International Electric Machines and Drives Conference, Miami, Florida, USA*, pp. 1844-1850, May 2009.

[8]   T. A. Haskew, *et al.*, "Characteristic Study of Vector Controlled Direct Driven Permanent Magnet Synchronous Generator in Wind Power Generation," *IEEE Power and Energy Society General Meeting - Conversion and Delivery of Electrical Energy in the 21st Century, Piscataway, NJ, USA*, pp. 1-9, Jul. 2008

[9]   A. Rolan, *et al.*, "Modeling of a Variable Speed Wind Turbine with a Permanent Magnet Synchronous Generator," *IEEE International Symposium on Industrial Electronics. Seoul, Korea*, pp. 734-739, Jul. 2009.

[10] A. Bendaikha, *et al.*, "Comparative Study of Five-Level and Seven-Level Inverter Controlled by Space Vector Pulse Width Modulation , " *International Journal of Power Electronics and Drive System (IJPEDS)*, pp. 755-766, Vol. 8, No. 2, June 2017.

[11] I. Huzainirah, *et al.*, "Constant Switching Frequency and Torque Ripple Minimization of DTC of Induction Motor Drives with Three-level NPC Inverter, " *International Journal of Power Electronics and Drive System (IJPEDS)*, pp. 1035-1049, Vol. 8, No. 3, September 2017.

[12] Saidah, *et al.*, "Control Strategy for PWM Voltage Source Converter Using Fuzzy Logic for Adjustable Speed DC Motor," *International Journal of Power Electronics and Drive System (IJPEDS),* pp. 51-58, Vol. 8, No. 1, March 2017.

[13] M. Depenbrok, "Direct self controlof inverter fed induction machine, " *IEEE Tans. Power Electron*, vol.3, pp. 420-429, 1988.

[14] Z. Xu, *et al.*, "Instantaneous torque control of a permanent magnet wind power generator without a position sensor," *IEEE International Conference on Electrical Machines and Systems, Wuhan, China*, pp. 1343-1347, Oct. 2008.

[15] B. Bossoufi1, *et al.*, "Low-Speed Sensorless Control of DFIG Generators Drive for Wind Turbines System", E-ISSN: 2224-2856- Volume 9, 2014.

[16] F. D. Bianchi, *et al.*, "Wind Turbine Control Systems: Principles, Modelling and Gain Scheduling Control," *Springer-Verlag London Limited,* 2007.

[17] O. Ouledali, *et al.*, "Direct Torque Fuzzy Control of PMSM based on SVM,*" Volume 74*, Pages 1314-1322*,* August 2015.

[18] F. Longfei, *et al.*, "Simulation Research on Direct Torque Control for Brushless DC Motor, " *International Conference on Intelligent Systems Research and Mechatronics Engineering (ISRME),* China, 2015.

[19] K. Chikh, *et al.*, "A Constant Switching Frequency DTC for PMSM Using Low Switching Losses SVM-An Experimental Result, " *International Journal of Power Electronics and Drive System (IJPEDS)),* pp. 558-583, Vol. 8, No. 2, June 2017.

[20] N.El Ouanjli, *et al.*, "Contribution to the Performance Improvement of Doubly Fed Induction Machine Functioning in Motor Mode by the DTC Control," *International Journal of Power Electronics and Drive System (IJPEDS),* Vol. 8, No. 3, pp. 1117-1127, September 2017.